Heliyon 10 (2024) e34399

Contents lists available at ScienceDirect

Heliyon

journal homepage: www.cell.com/heliyon

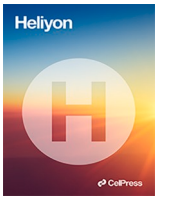

Research article

A depression-related lncRNA signature predicts the clinical outcome and immune characteristics of gastric cancer

Biao Ning [a,b,c], Tianhe Huang [a,b,c], Yixin Liu [a,b,c], Yongchang Wei [a,b,c,*]

[a] Department of Radiation and Medical Oncology, Zhongnan Hospital of Wuhan University, 169, Donghu Road, Wuchang District, Wuhan, Hubei Province, 430071, China
[b] Hubei Key Laboratory of Tumor Biological Behaviors Zhongnan Hospital of Wuhan University, 169, Donghu Road, Wuchang District, Wuhan, Hubei Province, 430071, China
[c] Hubei Cancer Clinical Study Center Zhongnan Hospital of Wuhan University, 169, Donghu Road, Wuchang District, Wuhan, Hubei Province, 430071, China

ARTICLE INFO

Keywords:
Gastric cancer
Depression
lncRNA
Risk model
Immunotherapy

ABSTRACT

Background: Depression and long non-coding RNA (lncRNA) have been reported to be associated with tumor progression and prognosis in gastric cancer (GC). This study aims to build a GC risk classification and prognosis model based on depression-related lncRNAs (DRLs).
Methods: To develop a risk model, we performed univariate Cox regression and least absolute shrinkage and selection operator (LASSO) regression analyses using RNA sequencing data of GC from The Cancer Genome Atlas (TCGA) and depression-related genes (DRGs) from previous studies. Kaplan-Meier analysis, receiver operating characteristic (ROC) curve analysis, nomogram construction, pathway enrichment analysis, assessment of immunological features, and drug sensitivity testing were conducted using a series of bioinformatics methods.
Results: Seven DRLs were identified to build a prognostic model, whose robustness was verified in an internal cohort. Subsequent prognostic analyses found that high risk scores were associated with worse overall survival (OS). Univariate and multivariate analyses revealed that the risk score could be used as an independent prognostic factor. Furthermore, the ROC curve indicated that the risk score had higher diagnostic efficiency than traditional clinicopathological features. The calibration curve confirmed the accuracy and reliability of the nomogram. Gene ontology (GO) and Kyoto Encyclopedia of Genes and Genomes (KEGG) enrichment analyses showed that there were differences in digestive system and nervous system-related pathways between the high- and low-risk groups. Results of tumor mutational burden (TMB) and tumor immune dysfunction and exclusion (TIDE) analyses indicated that patients in the low-risk group had a better response rate to immunotherapy. Finally, the results of drug sensitivity analysis showed that risk score could influence sensitivity to EHT 1864 in GC.
Conclusion: We have successfully developed and verified a 7-DRL risk model which can assess the prognosis and immunological features and guide individualized therapy of GC patients.

* Corresponding author. Department of Radiation and Medical Oncology, Zhongnan Hospital of Wuhan University, 169, Donghu Road, Wuchang District, Wuhan, Hubei Province, 430071, China.
E-mail addresses: 2016302180139@whu.edu.cn (B. Ning), tianhe2060@163.com (T. Huang), lyx19960626@163.com (Y. Liu), weiyongchang@whu.edu.cn (Y. Wei).

https://doi.org/10.1016/j.heliyon.2024.e34399
Received 29 July 2023; Received in revised form 29 June 2024; Accepted 9 July 2024
Available online 10 July 2024

1. Introduction

Gastric cancer (GC) was the fifth most common cancer and the fourth leading cause of cancer-related death globally, with more than one million new GC patients and nearly 0.77 million deaths reported in 2020 [1]. Currently, the predominant treatment options for GC include surgery, chemoradiotherapy, targeted therapy, and immunotherapy [2]. While these treatments have improved patient survival rates, the 5-year overall survival (OS) remains at a low level [3]. Besides, early symptoms of GC are often nonspecific, leading to a low early detection rate. Consequently, a large number of patients are detected at an advanced stage, which is one of the main reasons for the poor prognosis of GC [4]. The AJCC TNM staging system is mainly used to evaluate the prognosis of tumor patients and guide clinical treatment strategies [5]. However, due to high tumor heterogeneity, GC patients with the same stage and receiving similar therapy may have significantly different clinical outcomes [6]. Therefore, it is crucial to identify diagnostic and prognostic biomarkers that can accurately predict the prognosis of GC and offer new, effective treatment strategies. Therefore, it is very promising to discover and identify a new diagnostic and prognostic biomarker which can accurately predict prognosis and provide reference for clinical treatment of GC patients.

Depression is widely recognized as one of the most common mental illnesses, significantly negatively impacting patients' mental health and state of daily living. Currently, depression is one of the leading causes of the global burden of disease, imposing substantial personal, societal, and economic burdens [7]. It is reported that cancer patients have a higher incidence of depression than the general population [8]. Additionally, previous research has indicated that comorbid depression may be associated with poor prognosis and increased mortality in tumor patients [9–11]. Meanwhile, evidence shows that over 57 % of GC patients score high on depression scales [12,13]. GC patients with depression may experience worsening symptoms, reduced quality of life, and worse survival rates [14].

Recent studies have reported that depression affects endocrine function, inflammation, oxidative stress, immune function, and other biobehavioral pathways in cancer patients [15,16]. Similar findings have been observed in GC. For instance, Pan et al. demonstrated that depression could induce neuroendocrine phenotypes through β2-AR/MACC1 axis, promoting GC progression and metastasis [17]. Additionally, a recent review highlighted the importance of depression-induced reactive oxygen species (ROS) in GC. High levels of ROS could activate ABL1, facilitating the progression of GC [18]. Therefore, depression plays a crucial role in the progression and prognosis of GC.

Long non-coding RNA (lncRNA), with more than 200 nucleotides, affects cell differentiation and growth, gene expression, and chromatin organization formation [19,20]. On one hand, lncRNA plays a significant role in the pathogenesis of depression and can regard as a potential therapeutic target and a diagnostic biomarker for the condition [21]. On the other hand, lncRNA, as a diagnostic and prognostic biomarker for GC, has been studied in more and more projects for early diagnosis, evaluation of prognosis and drug response [22,23]. However, the value of depression-related lncRNA (DRL) in assessing the prognosis of GC patients hasn't been fully and effectively studies. Thus, this study aims to build a DRL-based prognostic model that can enhance current strategies for the diagnosis, treatment, and prevention of GC.

In this study, we constructed a new risk prognostic model based on the screened DRLs and verified its accuracy in assessing the prognosis of GC patients. As a result, it was confirmed that risk score was closely correlated with OS and progression-free survival (PFS). Additionally, our study showed that patients with low-risk scores responded better to immunotherapy. Moreover, EHT 1864 emerged as a potential targeted drug for the therapy of GC patients. To sum up, our study not only provides a novel prognostic model for evaluating GC prognosis but also underscores the clinical significance of assessing depression in GC treatment.

2. Materials and methods

2.1. Data collection and preparation

We downloaded gene expression data and clinicopathological features of GC patients from TCGA database (https://tcga-data.nci.nih.gov/tcga/). The RNA sequencing data was annotated and then distinguished into mRNAs and lncRNAs through Perl software. After excluding patients with absent prognostic information, we merged the lncRNA expression data with 438 patients' clinical data. Ultimately, 371 GC patients were included in the later analysis. These patients were randomly assigned to training (n = 186) and test sets (n = 185) using the R package "caret". Then, we obtained three gene lists which were thought to be associated with depression from previous studies [24–26]. The detailed gene names in the three lists were listed in Supplementary Table S1. These studies conducted genome-wide association meta-analysis based on over one million depression cases and controls, ensuring the authenticity of the results. Finally, thirty-eight depression-related genes (DRGs) were screened out by Venn diagram. The detailed names of the thirty-eight DRGs were listed in Supplementary Table S2.

2.2. Identification of depression-related LncRNAs

We eliminated samples with incomplete clinicopathological features, and then transformed Ensemble gene IDs into Gene symbol IDs. For genes with multiple gene symbols, we took the average value utilizing the "avereps" function of"limma" package [27]. The expression values of thirty-eight DRGs were extracted from GC gene expression matrix. Pearson correlation tests were then performed to identify eligible DRLs based on the screening criteria $|R| \geq 0.4$ and $p < 0.001$. A total of 631 DRLs co-expressed with DRGs were screened out. These lncRNAs were used for subsequent model construction. Finally, the co-expression of DRGs and DRLs was visualized utilizing a Sankey diagram created with the "ggplot2" and "ggalluvial" packages [28].

2.3. Construction of risk model

As previously mentioned, patients were randomly assigned into the training and the test set. We used the training set to build the prognostic model which was then verified the accuracy in the test set. We obtained nine DRLs ($p < 0.05$) associated with the OS of GC by using univariate Cox regression analysis. Furthermore, LASSO regression analysis was performed to avoid overfitting and to identify lncRNAs truly related to patient survival, based on 10-fold cross-validation. Multivariate Cox regression analysis identified seven DRLs to build a more robust prognostic model. Based on the seven optimal lncRNAs identified, the formula for the risk score of the prognostic signature was constructed as follows: $\sum_{i=1}^{n} Coef(i) \times x(i)$, where Coef(i) represented the coefficient of multiple Cox regression analysis of seven lncRNAs and x(i) indicated the expression level of each lncRNA. Based on the above formula, we calculated the risk score of all GC patients, and divided them into high- and low-risk groups according to the median risk score.

2.4. Assessment of prediction accuracy and independence of risk model

Kaplan-Meier analysis was utilized to evaluate OS and PFS between the two groups in the total set. The "pheatmap" package was employed to map patient survival status and lncRNA expression heatmaps based on the risk scores. Cox regression analysis was used to decide if the risk score could be used as an independent prognostic factor, and results were visualized using forest maps. Besides, the area under ROC curve for 1-year, 3-year, and 5-year OS, along with C-index curve, were utilized to assess the specificity and sensitivity of the model. Furthermore, patients were assigned into subgroups based on gender (Female and Male) and cancer stage (stages I–II and stages III–IV) to decide whether the prognostic risk score was applicable across different genders and stages of GC. Finally, we verified the reliability and accuracy of the model in an internal validation queue.

2.5. Establishment of the nomogram and functional enrichment analysis

A nomogram is a graphical tool that can quickly perform complex calculations [29]. We further utilized the package "rms" to build a nomogram, combining the risk score with clinicopathological characteristics to assess the predictive effect of the risk scores for 1-year, 3-year, and 5-year OS. A calibration plot was then generated to establish a concordance index, evaluating the accuracy of the nomogram's prediction results. The closer the calibration curve was to the diagonal, the better the prognostic predictive ability of the nomogram. We used the "limma" package for differential expression analysis, and obtained the differentially expressed genes (DEGs) between the two groups based on the screening criteria of $|\log2FoldChange| > 0.6$ and $p < 0.05$. We then performed GO and KEGG enrichment analyses to explore specific enrichment pathways and biological functions enriched in DEGs. The GO and KEGG analyses were carried out utilizing R packages such as "ggplot2," "enrichplot," "circlize," "org.Hs.eg.db," and "clusterProfiler."

2.6. Prediction of immunotherapy responsiveness and targeted drug sensitivity

The "limma", "pheatmap", "GSVA", and "reshape2″ R packages were used to generate heatmap to demonstrate the activity of 13 immune-related functions and to compare differences between high- and low-risk groups. Tumor mutational burden (TMB) data were also derived from TCGA database, and each patient's TMB score was calculated. The TBM values in the two groups were compared using *t*-test. In addition, the "limma" and "ggpubr" packages were utilized to demonstrate the relationship between TMB and OS. TMB and risk scores were integrated and survival curves were plotted. The mutation profiles and frequencies of genes in the two groups were explored and visualized utilizing package "maftools". To predict the treatment outcome to immunotherapy, the tumor immune dysfunction and exclusion (TIDE, http://tide.dfci.harvard.edu/) algorithm was established and the "limma" and "ggpubr" packages were utilized to compare differences between the two groups [30]. Finally, to better apply the model to clinical practice, the R package "pRRophetic" was used to predict the half-maximal inhibitory concentrations (IC50) of potential drugs [31]. A p-value <0.001 was regarded as statistically significant.

2.7. Statistical analysis

R software (version 4.1.2) was used for statistical analysis and graph drawing. Data processing was primarily performed using Perl software (version 5.30.0.1). Kaplan-Meier analysis was employed to compare OS and PFS between the two groups. Differences between subgroups were analyzed using *t*-test and the Wilcoxon signed-rank test. Unless otherwise stated, p-value was bilateral, and $p < 0.05$ was regarded as statistically significant.

3. Results

3.1. Construction of Seven-DRLs risk model

To ensure the genes were related to depression, a Venn diagram was drawn to select the overlapped genes from all three gene lists. Thirty-eight genes were screened out and defined as depression-related genes (DRGs) (Fig. 1A). Then we identified a total of 631 DRLs associated with these 38 DRGs through Pearson correlation analysis (Supplementary Table S3). The results of co-expression were presented using Sankey diagram (Fig. 1B).

In this study, TCGA GC cases were randomly segregated into training set of 186 cases and test set of 185 cases. The details of clinical characteristics for the training, test, and total set were listed in Table 1. To identify DRLs related to OS, we executed univariate Cox regression analysis and identified 9 prognostic DRLs (Fig. 1C). Subsequently, LASSO regression analysis was utilized to avert overfitting, selecting 8 DRLs (Fig. 1D and E). Multivariate Cox regression analysis further confirmed 7 DRLs to construct the risk model. The risk scoring formula was constructed according to the calculated Cox regression coefficients and lncRNA expression values: Risk score = AP003392.1 × (−0.9253) + AC068790.7 × (2.1807) + CCNT2-AS1 × (1.3812) + IPO5P1 × (−1.0032) + AC129507.1 × (1.4003) + AL160006.1 × (−1.2747) + AC103736.1 × (1.4903). Then, the correlation heatmap further summarized the correlations between the 7 DRLs and the 38 DRGs (Fig. 1F). Notably, ZSCAN12, ZNF660, ZNF445, ZKSCAN8, ZKSCAN7, PGBD1, PAX5, and KLC1 showed positive correlations with all 7 DRLs.

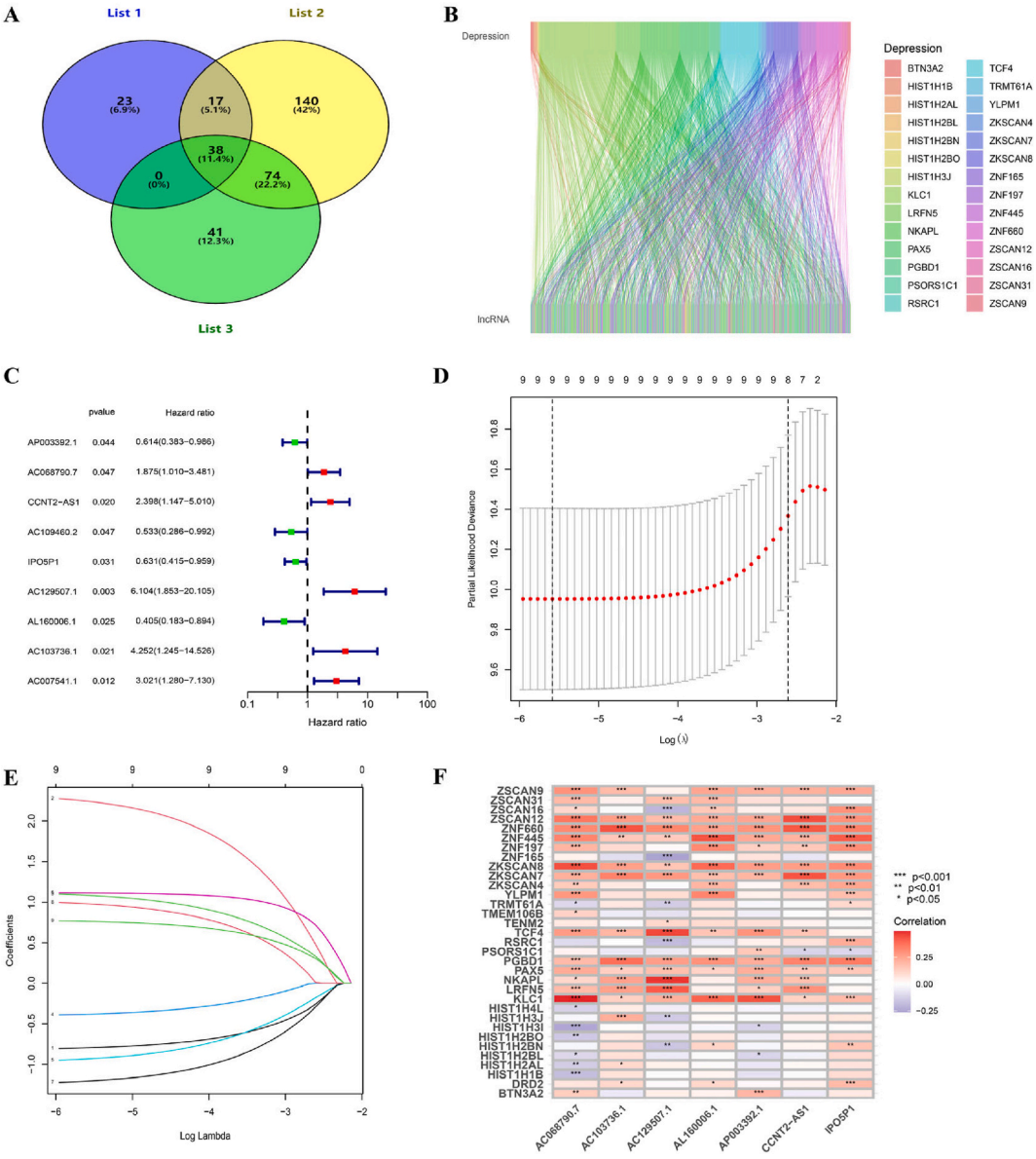

Fig. 1. Identification of DRL based prognostic signature in GC. (A) Venn diagram containing three lists of depression-related genes. (B) Sankey relationship diagram of depression genes and DRLs. (C) Univariate COX regression analysis to select prognostic lncRNAs. (D, E) LASSO Cox regression with a 10-fold cross-validation for the prognostic value of the DRLs. (F) Correlation of lncRNAs with depression-related genes in risk models.

Table 1
Clinical information of the total set, test set and training set.

Covariates	Type	Total	Test	Train	P value
Age	≤65	163(43.94 %)	84(45.41 %)	79(42.47 %)	0.6747
	>65	205(55.26 %)	100(54.05 %)	105(56.45 %)	
	unknow	3(0.81 %)	1(0.54 %)	2(1.08 %)	
Gender	FEMALE	133(35.85 %)	70(37.84 %)	63(33.87 %)	0.4912
	MALE	238(64.15 %)	115(62.16 %)	123(66.13 %)	
Grade	G1	10(2.7 %)	7(3.78 %)	3(1.61 %)	0.3598
	G2	134(36.12 %)	68(36.76 %)	66(35.48 %)	
	G3	218(58.76 %)	104(56.22 %)	114(61.29 %)	
	unknow	9(2.43 %)	6(3.24 %)	3(1.61 %)	
Stage	Stage I	50(13.48 %)	20(10.81 %)	30(16.13 %)	0.5022
	Stage II	111(29.92 %)	57(30.81 %)	54(29.03 %)	
	Stage III	149(40.16 %)	77(41.62 %)	72(38.71 %)	
	Stage IV	38(10.24 %)	20(10.81 %)	18(9.68 %)	
	unknow	23(6.2 %)	11(5.95 %)	12(6.45 %)	

3.2. Validation of the DRL risk model

The risk scores of all patients were calculated according to the risk scoring formula. The median risk score of patients in the training set was defined as a cut-off value, according to which patients were divided into high- and low-risk groups. To evaluate whether risk score could accurately predict prognosis for GC patients, we conducted Kaplan-Meier analysis to generate survival curves for training, test, and total set, respectively. The results showed that patients with higher risk scores had significantly shorter OS across all three datasets (Fig. 2A–C). Furthermore, PFS evaluated in the total set revealed that PFS appeared shorter in high-risk group (Fig. 2D). The

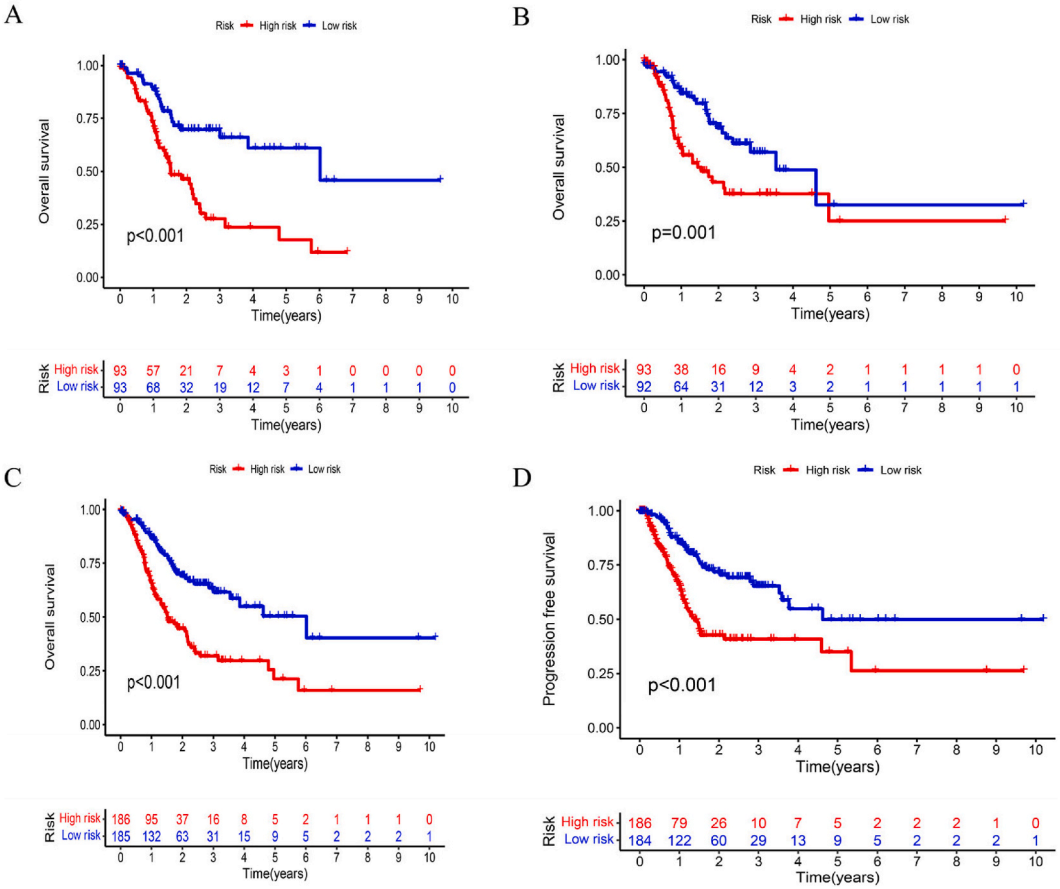

Fig. 2. Survival analysis of the high- and low-risk groups in GC patients. (A) K-M survival curve on OS status of training set in GC patients. (B) K-M survival curve on OS status of test set in GC patients. (C) K-M survival curve on OS status of total set in GC patients. (D) K-M survival curve on PFS status of total set in GC patients.

combined analysis of risk score and survival status showed that GC patients in low-risk group had lower mortality and risk score across all three datasets (Fig. 3A and B). A heatmap generated from the expression data of 7 DRLs in the two groups showed similar expression patterns across the three sets (Fig. 3C). For example, AC068790.7, CCNT2-AS1, AC129507.1, and AC103736.1 were regarded as high-risk lncRNAs, whereas AP003392.1, IPO5P1, and AL160006.1 were regarded as low-risk lncRNAs.

3.3. Independent prognostic analysis of risk model

We used univariate and multivariate Cox regression analyses to determine whether risk score could be regarded as an independent prognostic factor. Univariate Cox regression analysis indicated that risk score (HR = 1.104, $p < 0.001$) could be used as a predictor of OS (Fig. 4A). Multivariate Cox regression analysis further clarified that risk score (HR = 1.119, $p < 0.001$) continued to have a significant effect on OS (Fig. 4B). These findings demonstrated that risk score could be regarded as an independent prognostic factor in patients with GC, independent of other clinicopathological features.

Moreover, time-dependent ROC curves were used to evaluate the predictive power of the model, with 1-year, 3-year, and 5-year AUC values of 0.736, 0.686, and 0.715, respectively (Fig. 4C). The clinical ROC curves were created by integrating risk score with clinical indicators (Fig. 4D), and it was found that the AUC value of risk score was the highest, which proved that the prediction efficiency of the risk score was the best. The C-index curve results corroborated these findings (Fig. 4E). To better assess predictive accuracy, the analyses were replicated in both the training set (Supplementary Figs. S1A–D) and the test set (Supplementary Figs. S2A–D). Cox regression analyses confirmed that risk score was an independent prognostic factor. ROC curves demonstrated that AUC value of risk score was higher than other clinicopathological indicators.

Kaplan-Meier survival analyses were performed in different clinical subgroups to assess the stability of risk score in predicting prognosis. Among the total set patients stratified by sex (female and male) and disease stage (stages I-II and III-IV), high-risk patients had significantly shorter OS than patients in the low-risk group (Supplementary Figs. S3A–D). These results indicated that the prognostic model could accurately predict prognosis and effectively evaluate OS in GC patients across different genders and stages. All above results guaranteed the credibility and practicality of our model.

3.4. Construction of a nomogram and functional enrichment analysis

To further verify the accuracy of this prognostic model in predicting the prognosis of GC patients, we built a nomogram through integrating clinicopathological features and risk scores to forecast 1-year, 3-year, and 5-year OS (Fig. 5A). Calibration curve was used to verify the predictive power of the nomogram and the results showed that the OS predicted through the nomogram was consistent with the actual OS (Fig. 5B). Thus, the nomogram was well-calibrated and provided reliable predictions of patient OS.

We have verified that the DRL-based prognostic model had high specificity and accuracy in predicting the prognosis of GC patients, and then we continued to explore its potential mechanism. First, effective DEGs were screened out between high - and low-risk groups based on the screening criteria outlined in the method section. To elucidate the biological functions which risk score could influence, we performed GO and KEGG enrichment analyses based on DEGs (Fig. 5C and D). The results of biological process (BP) enriched in“regulation of hormone levels”, “digestion”, “digestive system process”, and “phospholipase C-activating G protein-coupled receptor signaling pathway”; Cellular component (CC) mainly focused on “neuronal dense core vesicle”; Molecular function (MF) enriched

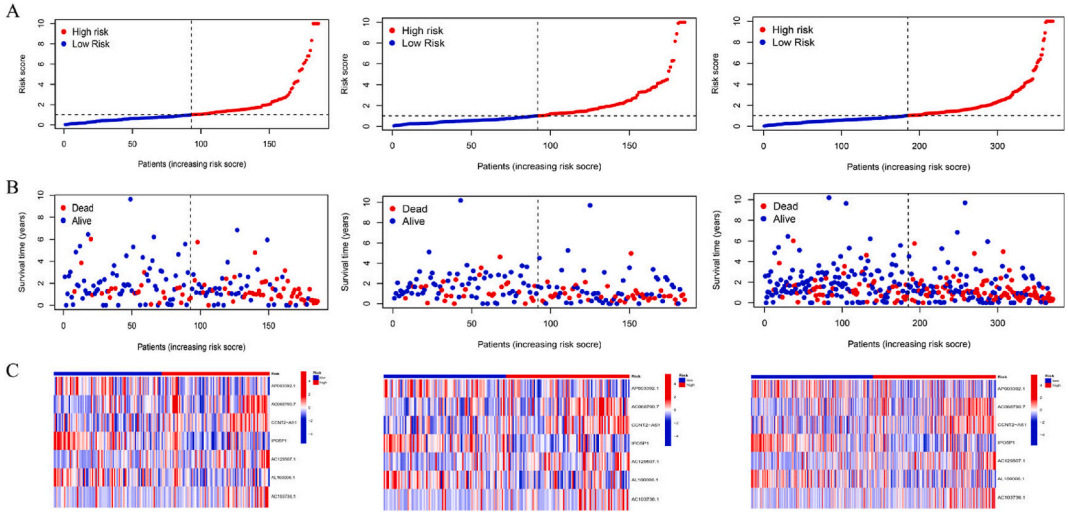

Fig. 3. Risk curve analysis of the training, test and total set (from left to right). (A) Risk score distribution of patients with GC based on DRLs. (B) Scatter plots showed the association between the OS and the risk score distribution. (C) Heat maps of expression of the seven lncRNAs signals associated with depression.

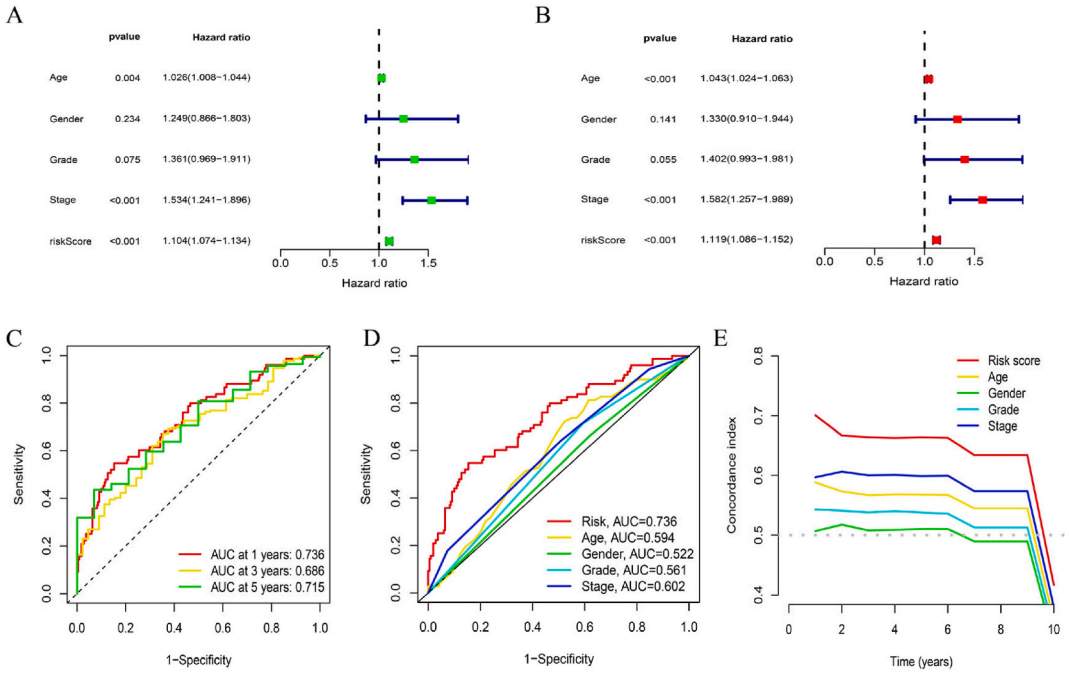

Fig. 4. Evaluation of the prognostic DRL signature in total set. (A) Forest plot for univariate Cox regression analysis. (B) Forest plot for multivariate Cox regression analysis. (C) The ROC curve predicted 1, 3, and 5 years of OS for GC patients. (D) ROC demonstrated the predictive accuracy of the risk model was superior to other clinicopathological variables. (E) C-index showed the predictive accuracy of the risk model was superior to other clinicopathological variables.

in"signaling receptor activator activity", "receptor ligand activity", and "G protein-coupled receptor binding". More importantly, KEGG was enriched in "Protein digestion and absorption", "Pancreatic secretion", "Neuroactive ligand-receptor interaction", "Renin-angiotensin system", and "Gastric acid secretion". As a result, all the biological functions mentioned above were all involved in the digestive system and the nervous system, which indicated that our risk score could serve as a predictive marker of digestive and nervous function for GC patients.

3.5. Analysis of immunotherapy response and drug sensitivity

GSVA enrichment analysis was used to assess whether risk score could affect the function of immune-related pathways. The heatmap showed that the function of type I and type II IFN response pathways in high-risk group differed significantly from that in low-risk group, while this difference was not observed in other pathways (Fig. 6A). In addition, we assessed whether there was an association between TMB and risk score. The result showed a significant difference in TMB values between the two groups (Fig. 6B). We further found that low TMB was associated with shorter OS (Fig. 6C). To further assess the synergism of risk score and TMB in predicting outcome in GC patients, we performed a stratified survival curve analysis of these two markers. As shown in Fig. 6D, TMB value did not influence the prognostic power of the risk score, and the longest OS was observed in the high-TMB + low-risk group.

In addition, we used the maftools algorithm to probe and visualize gene mutations in different risk groups. The integrated landscape of somatic variations depicted mutational patterns of the 20 driver genes with the highest mutation frequency (Fig. 6E and F). The results revealed a higher frequency of mutations in low-risk group compared to high-risk group (TTN: 52 % versus 48 %; MUC16: 34 % versus 26 %; ARID1A: 33 % versus 20 %). These findings provided new insights into the intrinsic association between risk score and somatic variation in immunotherapy of GC. Subsequently, we used TIDE scores to assess the response of different risk groups to immune checkpoint inhibitors (ICIs). Interestingly, we observed a higher TIDE value in high-risk group, indicating a greater immune escape capacity and a subsequent less favorable outcome of immunotherapy (Fig. 7A). Overall, these findings suggested that risk scores may hold potential for assessing the clinical outcome of anti-tumor immunotherapy.

In addition to immunotherapy, we further investigated whether risk scores could influence the efficacy of chemotherapy and targeted therapeutic agents for GC. It is well known that IC50 value is positively correlated with drug sensitivity. Ultimately, we identified 17 drugs whose sensitivity differed significantly between the two risk groups ($p < 0.001$), one of which was EHT 1864 (Fig. 7B-R). These findings provide an important reference for the potential clinical value of these drugs in treatment of GC.

4. Discussion

GC stands as one of the most prevalent malignant tumors worldwide. Despite advancements in both economy and medical

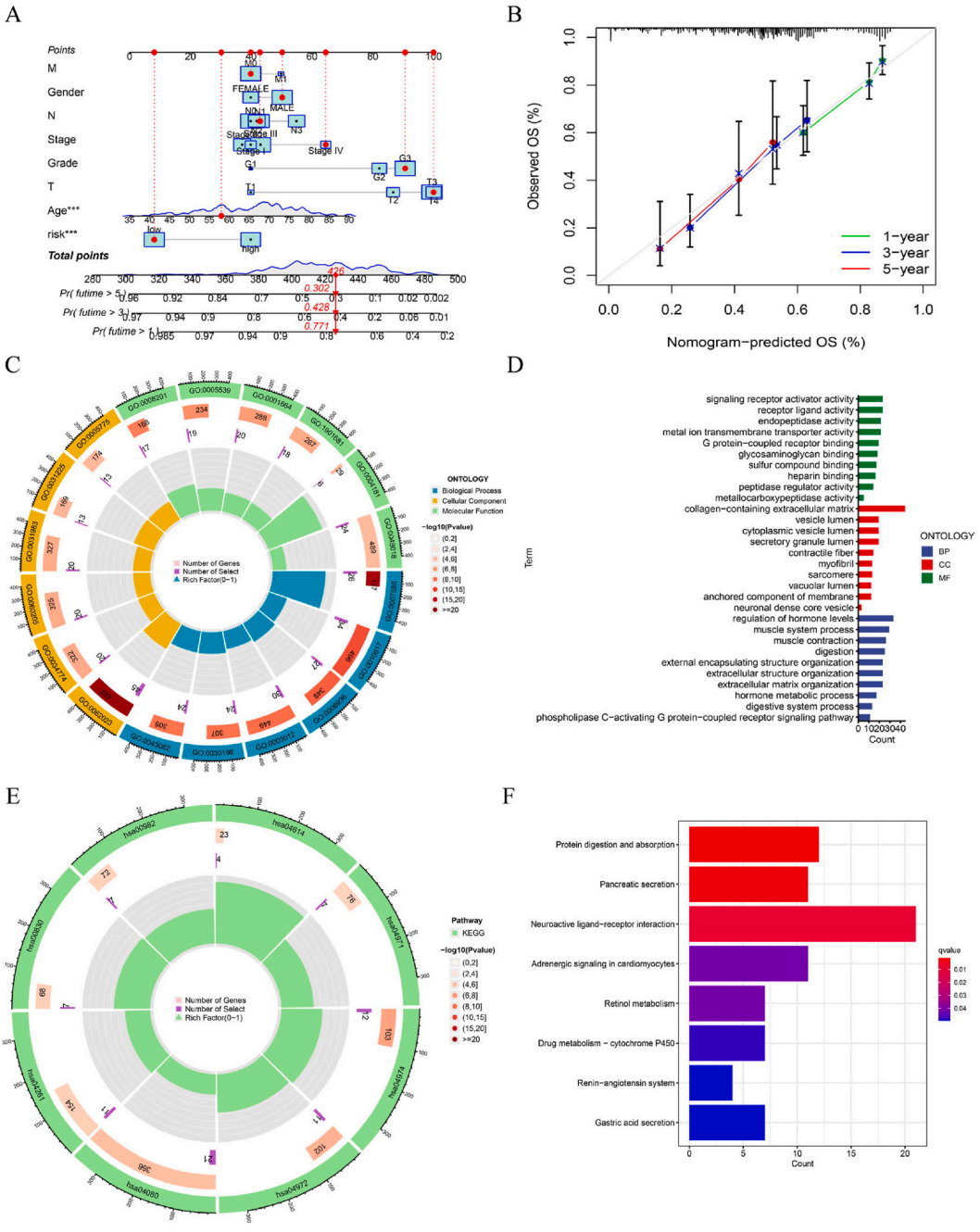

Fig. 5. Construction and validation of the nomogram and pathway enrichment analysis. (A) Nomogram with Risk scores and clinicopathological features for risk score calculation. (B) Calibration plots for 1-, 3-, and 5-years survival predictions. (C) Circle diagram of GO enrichment analysis. (D) Barplot of the top 10 GO enrichment terms. (E) Circle diagram of KEGG enrichment analysis. (F) Barplot of the top 8 KEGG enrichment terms.

technology, the 5-year OS of advanced GC patients remains around 20 % [32,33]. The heterogeneity of GC leads to varying responses to similar therapies and distinct OS rates among patients, even with the same pathologic and TNM stages. Hence, there's a pressing need to identify highly specific and sensitive methods for early screening and identification of high-risk patients to enhance GC patient's outcomes. Additionally, the development of reliable prognostic factors for GC is imperative. Recent studies indicated that cancer patients, including those with GC, were more susceptible to depression [34]. Evidence suggested that individuals with GC had a higher incidence of depression compared to the general population [35]. Moreover, recent research had highlighted the negative correlation between the incidence and severity of depression and DFS and OS in GC patients [36]. Thus, it is promising to explore the link between depression and GC. As we all know, lncRNAs play multifaceted roles in the occurrence, progression, and metastasis of GC

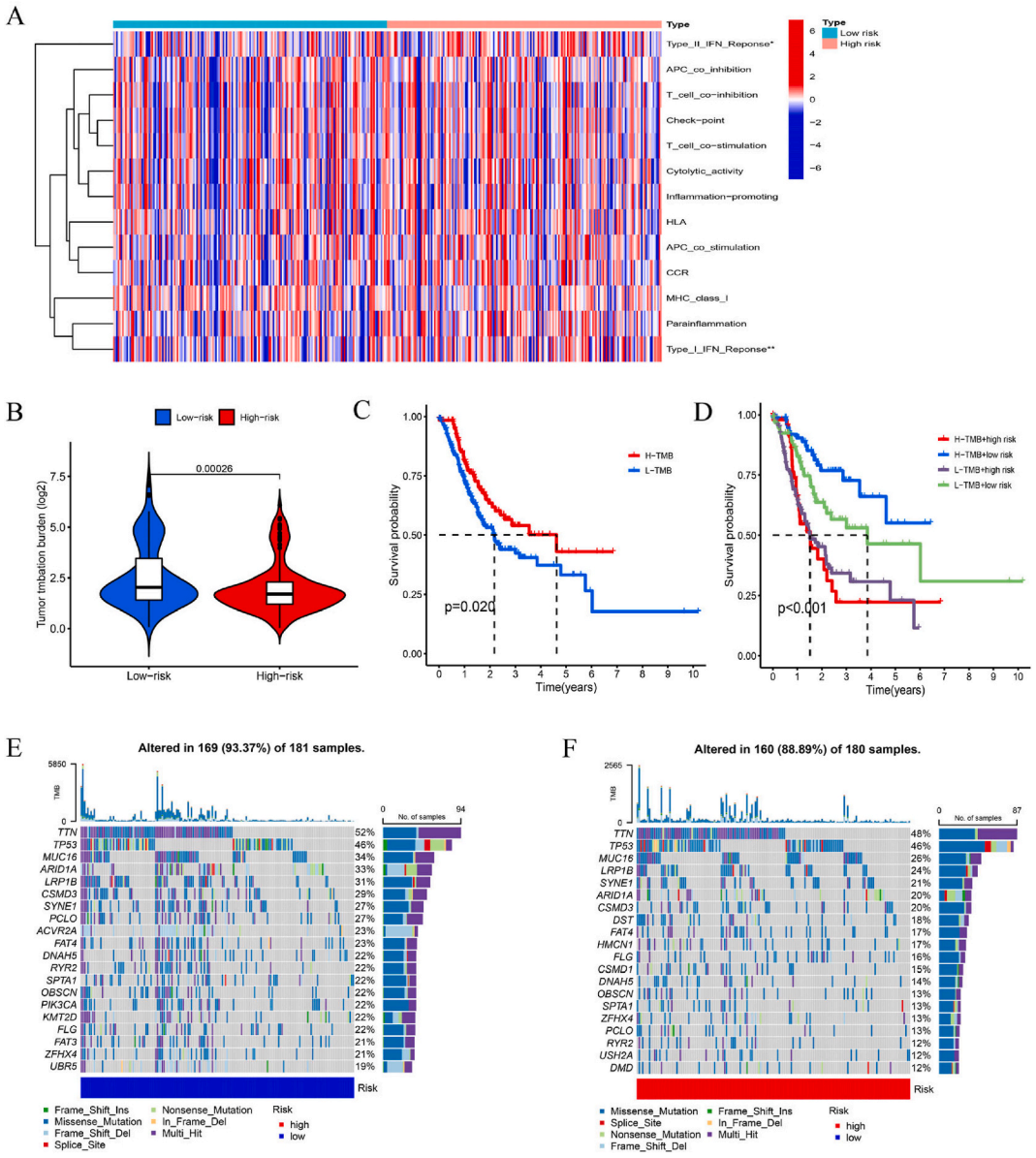

Fig. 6. Immune related analysis and relationship between TMB and the signature. (A) Immune-related function analysis in low- and high-risk groups. (B) TMB between the low- and high-risk groups. (C) Survival analysis curves of the high- and low-TMB groups. (D) K–M survival curves between the four groups. (E) Waterfall plot revealed the top 20 mutation genes in GC for the low-risk (181 samples) group. (F) Waterfall plot revealed the top 20 mutation genes in GC for the high-risk (180 samples) group. "*" represents p value < 0.01.

[22,37–40]. And multiple lncRNA prognostic models can evaluate the OS of GC [41–44]. However, lncRNAs associated with depression have not been explored in the context of GC. Therefore, establishing a risk model using DRLs in GC holds significant research importance and value.

In this research, we built a seven-DRLs risk model to improve diagnostic accuracy and predict the prognosis of GC patients. Initially, we retrieved the RNA sequencing data and corresponding clinical data of GC patients from TCGA. After screening and elimination, a cohort of 371 patients was identified and randomly partitioned into two sets. Subsequently, we identified 631 DRLs through co-expression analysis. Using LASSO and Cox regression analysis, we selected seven prognostic DRLs (AP003392.1, AC068790.7, CCNT2-AS1, IPO5P1, AC129507.1, AL160006.1, AC103736.1) to construct our risk model. Among these seven lncRNAs, AP003392.1, AC068790.7, and AC129507.1 were identified as risk factors for GC patients, consistent with previous results [45–47]. Additionally, CCNT2-AS1, IPO5P1, and AL160006.1 have been reported as components of risk models in other cancer types [48–50]. Notably, there is currently no relevant study regarding AC103736.1, warranting further analysis and investigation.

Subsequently, we evaluated the validity and reliability of our risk model. Using the risk score, GC patients were randomly stratified

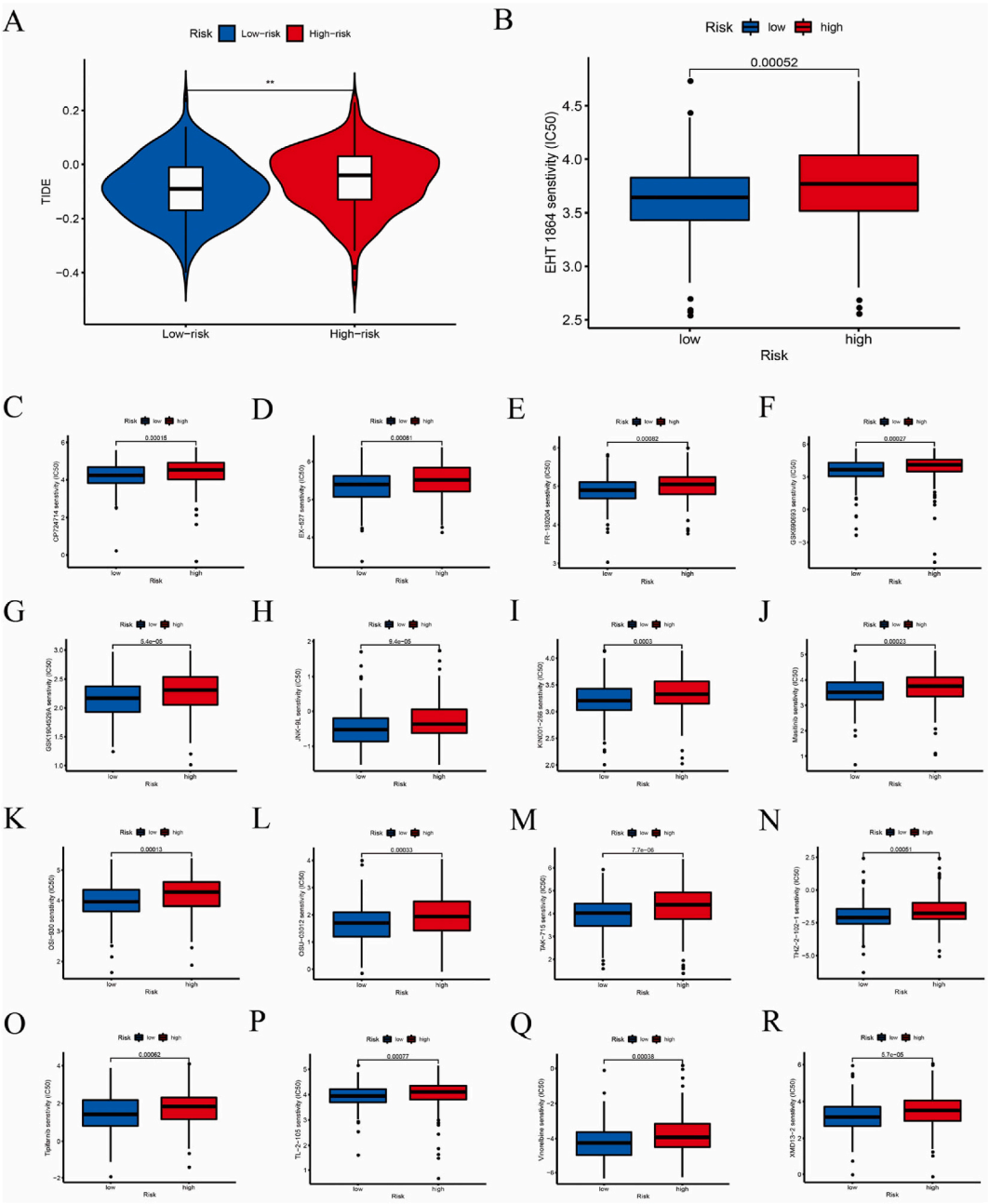

Fig. 7. Impact of signature on TIDE and drug sensitivity. (A) TIDE scoring for immune evasion in low- and high-risk groups. (B–R) 17 common drugs which exhibit different IC50 in two groups. "**" represents p value < 0.01.

into two groups based on the median risk score. Kaplan-Meier analysis showed that patients with low-risk values had longer OS and PFS. Furthermore, Cox regression analysis of risk score alongside clinical features confirmed that risk score could be used as an independent prognostic factor for GC patients. ROC curve and C-index curve indicated that risk score could accurately predict 1-, 3-, and 5-year OS. In addition, based on risk score and clinicopathological characteristics, a nomogram was developed to forecast the prognosis of GC patients. The calibration curve further verified that the predicted outcome of nomogram was consistent with the actual one. Further exploration via GO and KEGG enrichment analyses unveiled potential biological functions primarily related to digestive and nervous systems. This suggested that DRLs could bridge connections between the digestive and nervous systems, enhancing the prognostic prediction of GC patients, particularly those with depression.

Recent advancements in immunotherapy, particularly ICIs, have revolutionized the clinical landscape of GC treatment and prognosis [51]. TMB has emerged as a promising biomarker for predicting survival following immunotherapy across various cancer

types, with higher TMB associated with improved OS [52]. Consistent with previous findings, our study showed that patients with low-risk values possessed higher TMB and longer OS. However, it is crucial to acknowledge that immune escape constituted a primary challenge in tumor immunotherapy. To delve deeper into this phenomenon, we explored whether there were differences in the activity of immune-related pathways between different risk groups. Interestingly, we observed higher activity levels of type II and type I IFN responses in high-risk group. In previous studies, type I IFN and type II IFN could promote immune evasion among various cancer types [53,54]. We further performed TIDE analysis, where a higher TIDE score often indicated an enhanced immune escape ability. Our results revealed that high-risk patients exhibited higher TIDE scores compared to their counterparts. In summary, patients classified into the high-risk group exhibited a heightened risk of immune escape and a poorer response to immunotherapy. These findings underscore the importance of incorporating risk stratification approaches into the design and implementation of immunotherapeutic strategies for GC management.

In our drug sensitivity analysis, we identified EHT 1864 as having a significantly different IC50 between the two risk groups. EHT 1864 is a small-molecule inhibitor targeting Ras-related C3 botulinum toxin substrate 1 (Rac1), which functions by impeding Rac1 activation and consequently inhibiting downstream effector proteins [55]. Rac1 plays an important regulatory role in both GC and depression and has been extensively studied in various contexts [56–58]. Therefore, exploring the efficacy of EHT 1864 in GC patients with comorbid depression holds substantial significance for future research endeavors. This exploration may shed light on novel therapeutic strategies targeting Rac1 and its downstream pathways for improving outcomes in GC patients, particularly those with depression.

Indeed, our study has several limitations that warrant acknowledgment. Firstly, the risk model was developed solely utilizing retrospective data from the TCGA database, which may introduce inherent biases. Although the dataset included a substantial number of GC patients, the robustness of our findings could be further bolstered by external validation cohorts. Unfortunately, suitable external validation cohorts were not available at present. Secondly, the results of TMB and TIDE scores were extrapolated from RNA sequencing data. Thus, the predictive power of our risk score for immunotherapy efficacy required validation in future immunotherapy cohorts, preferably utilizing clinical data directly assessing TMB and immune checkpoint expression. Lastly, while our study identified potential molecular markers of DRLs in GC, further experimental validation in in vivo and in vitro models is essential to elucidate the precise molecular mechanisms underlying their roles in GC pathogenesis and progression.

5. Conclusion

In this study, we successfully built a robust risk model utilizing seven DRLs, enabling accurate prognostic predictions for GC patients. Additionally, immune analysis underscored the sensitivity of ICIs in GC, while drug sensitivity analysis identified a novel targeted drug candidate. These findings hold promise in guiding clinical management and facilitating individualized therapy approaches for GC patients in the future.

Data availability statement

The datasets used and analyzed during the current study available from the corresponding author on reasonable request.

Ethnical statement

Informed consent was not required for this study because it is not involved any human experiments.

CRediT authorship contribution statement

Biao Ning: Writing – original draft, Visualization, Validation, Project administration, Methodology, Formal analysis, Data curation, Conceptualization. **Tianhe Huang:** Writing – review & editing, Supervision, Formal analysis. **Yixin Liu:** Software, Resources, Investigation. **Yongchang Wei:** Writing – review & editing, Supervision, Funding acquisition.

Declaration of competing interest

The authors declare that they have no known competing financial interests or personal relationships that could have appeared to influence the work reported in this paper.

Appendix A. Supplementary data

Supplementary data to this article can be found online at https://doi.org/10.1016/j.heliyon.2024.e34399.

Abbreviations

lncRNA	long non-coding RNA
GC	Gastric cancer
DRL	Depression-related lncRNA

DRG	Depression-related gene
DEG	Differentially expressed gene
TCGA	The Cancer Genome Atlas
ROC	Receiver operating characteristic
OS	Overall survival
ROS	Reactive oxygen species
PFS	Progression-free survival
GO	Gene Ontology
KEGG	Kyoto Encyclopedia of Genes and Genomes
IC50	half-maximal inhibitory concentrations
CC	Cellular component
MF	Molecular function
BP	Biological process
TMB	Tumor mutational burden
TIDE	Tumor immune dysfunction and exclusion
ICI	Immune checkpoint inhibitor

References

[1] H. Sung, J. Ferlay, R.L. Siegel, et al., Global cancer statistics 2020: GLOBOCAN estimates of incidence and mortality worldwide for 36 cancers in 185 countries, Ca - Cancer J. Clin. 71 (2021) 209–249.
[2] F.M. Johnston, M. Beckman, Updates on management of gastric cancer, Curr. Oncol. Rep. 21 (2019) 67.
[3] W. Zhao, M. Liu, M. Zhang, et al., Effects of inflammation on the immune microenvironment in gastric cancer, Front. Oncol. 11 (2021) 690298.
[4] M. Orditura, G. Galizia, V. Sforza, et al., Treatment of gastric cancer, World J. Gastroenterol. 20 (2014) 1635–1649.
[5] L.L. Zhang, F. Xu, D. Song, et al., Development of a nomogram model for treatment of nonmetastatic nasopharyngeal carcinoma, JAMA Netw. Open 3 (2020) e2029882.
[6] Y. Shao, Y. Geng, W. Gu, et al., Assessment of lymph node ratio to replace the pN categories system of classification of the TNM system in esophageal squamous cell carcinoma, J. Thorac. Oncol. 11 (2016) 1774–1784.
[7] Global Burden of Disease Study C, Global, regional, and national incidence, prevalence, and years lived with disability for 301 acute and chronic diseases and injuries in 188 countries, 1990-2013: a systematic analysis for the Global Burden of Disease Study 2013, Lancet 386 (2015) 743–800.
[8] M.B. Currier, C.B. Nemeroff, Depression as a risk factor for cancer: from pathophysiological advances to treatment implications, Annu. Rev. Med. 65 (2014) 203–221.
[9] G. Fervaha, J.P. Izard, D.A. Tripp, et al., Depression and prostate cancer: a focused review for the clinician, Urol. Oncol. 37 (2019) 282–288.
[10] C.F. Sharpley, D.R.H. Christie, V. Bitsika, Depression and prostate cancer: implications for urologists and oncologists, Nat. Rev. Urol. 17 (2020) 571–585.
[11] X. Wang, N. Wang, L. Zhong, et al., Prognostic value of depression and anxiety on breast cancer recurrence and mortality: a systematic review and meta-analysis of 282,203 patients, Mol. Psychiatr. 25 (2020) 3186–3197.
[12] G.M. Kim, S.J. Kim, S.K. Song, et al., Prevalence and prognostic implications of psychological distress in patients with gastric cancer, BMC Cancer 17 (2017) 283.
[13] A. Tavoli, M.A. Mohagheghi, A. Montazeri, et al., Anxiety and depression in patients with gastrointestinal cancer: does knowledge of cancer diagnosis matter? BMC Gastroenterol. 7 (2007) 28.
[14] H. Yu, Y. Wang, X. Ge, et al., Depression and survival in Chinese patients with gastric cancer: a prospective study, Asian Pac. J. Cancer Prev. APJCP 13 (2012) 391–394.
[15] B. Bortolato, T.N. Hyphantis, S. Valpione, et al., Depression in cancer: the many biobehavioral pathways driving tumor progression, Cancer Treat Rev. 52 (2017) 58–70.
[16] J.C. Zong, X. Wang, X. Zhou, et al., Gut-derived serotonin induced by depression promotes breast cancer bone metastasis through the RUNX2/PTHrP/RANKL pathway in mice, Oncol. Rep. 35 (2016) 739–748.
[17] C. Pan, J. Wu, S. Zheng, et al., Depression accelerates gastric cancer invasion and metastasis by inducing a neuroendocrine phenotype via the catecholamine/beta2 -AR/MACC1 axis, Cancer Commun. 41 (2021) 1049–1070.
[18] T. Huang, F. Zhou, F. Wang-Johanning, et al., Depression accelerates the development of gastric cancer through reactive oxygen speciesactivated ABL1 (Review), Oncol. Rep. 36 (2016) 2435–2443.
[19] E. Abdi, S. Latifi-Navid, F. Abdi, Z. Taherian-Esfahani, Emerging circulating MiRNAs and LncRNAs in upper gastrointestinal cancers, Expert Rev. Mol. Diagn. 20 (2020) 1121–1138.
[20] E. Abdi, S. Latifi-Navid, V. Kholghi-Oskooei, et al., Interaction between lncRNAs HOTAIR and MALAT1 tagSNPs in gastric cancer, Br. J. Biomed. Sci. 78 (2021) 147–150.
[21] W.Z. Hao, Q. Chen, L. Wang, et al., Emerging roles of long non-coding RNA in depression, Prog. Neuro-Psychopharmacol. Biol. Psychiatry 115 (2022) 110515.
[22] S. Ghafouri-Fard, M. Taheri, Long non-coding RNA signature in gastric cancer, Exp. Mol. Pathol. 113 (2020) 104365.
[23] L. Yuan, Z.Y. Xu, S.M. Ruan, et al., Long non-coding RNAs towards precision medicine in gastric cancer: early diagnosis, treatment, and drug resistance, Mol. Cancer 19 (2020) 96.
[24] D.M. Howard, M.J. Adams, T.K. Clarke, et al., Genome-wide meta-analysis of depression identifies 102 independent variants and highlights the importance of the prefrontal brain regions, Nat. Neurosci. 22 (2019) 343–352.
[25] D.M. Howard, M.J. Adams, M. Shirali, et al., Genome-wide association study of depression phenotypes in UK Biobank identifies variants in excitatory synaptic pathways, Nat. Commun. 9 (2018) 1470.
[26] N.R. Wray, S. Ripke, M. Mattheisen, et al., Genome-wide association analyses identify 44 risk variants and refine the genetic architecture of major depression, Nat. Genet. 50 (2018) 668–681.
[27] M.E. Ritchie, B. Phipson, D. Wu, et al., Limma powers differential expression analyses for RNA-sequencing and microarray studies, Nucleic Acids Res. 43 (2015) e47.
[28] S. Liu, X. Xie, H. Lei, et al., Identification of key circRNAs/lncRNAs/miRNAs/mRNAs and pathways in preeclampsia using bioinformatics analysis, Med. Sci. Monit. 25 (2019) 1679–1693.
[29] S.Y. Park, Nomogram: an analogue tool to deliver digital knowledge, J. Thorac. Cardiovasc. Surg. 155 (2018) 1793.
[30] P. Jiang, S. Gu, D. Pan, et al., Signatures of T cell dysfunction and exclusion predict cancer immunotherapy response, Nat. Med. 24 (2018) 1550–1558.
[31] P. Geeleher, N. Cox, R.S. Huang, pRRophetic: an R package for prediction of clinical chemotherapeutic response from tumor gene expression levels, PLoS One 9 (2014) e107468.

[32] S.H. Min, Y. Won, G. Kim, et al., 15-year experience of laparoscopic gastrectomy in advanced gastric cancer: analysis on short-term and long-term oncologic outcome, Surg. Endosc. 34 (2020) 4983–4990.
[33] K. Misawa, Y. Mochizuki, M. Sakai, et al., Randomized clinical trial of extensive intraoperative peritoneal lavage versus standard treatment for resectable advanced gastric cancer (CCOG 1102 trial), Br. J. Surg. 106 (2019) 1602–1610.
[34] M. Hernandez Blazquez, J.A. Cruzado, A longitudinal study on anxiety, depressive and adjustment disorder, suicide ideation and symptoms of emotional distress in patients with cancer undergoing radiotherapy, J. Psychosom. Res. 87 (2016) 14–21.
[35] S. Kwon, J. Kim, T. Kim, et al., Association between gastric cancer and the risk of depression among South Korean adults, BMC Psychiatr. 22 (2022) 207.
[36] L. Han, Prevalence, risk factors and prognostic role of anxiety and depression in surgical gastric cancer patients, Transl. Cancer Res. 9 (2020) 1371–1383.
[37] D. Fu, Y. Shi, J.B. Liu, et al., Targeting long non-coding RNA to therapeutically regulate gene expression in cancer, Mol. Ther. Nucleic Acids 21 (2020) 712–724.
[38] Y. Huang, J. Zhang, L. Hou, et al., LncRNA AK023391 promotes tumorigenesis and invasion of gastric cancer through activation of the PI3K/Akt signaling pathway, J. Exp. Clin. Cancer Res. 36 (2017) 194.
[39] G.H. Wei, X. Wang, lncRNA MEG3 inhibit proliferation and metastasis of gastric cancer via p53 signaling pathway, Eur. Rev. Med. Pharmacol. Sci. 21 (2017) 3850–3856.
[40] L. Zhang, W. Kang, X. Lu, et al., LncRNA CASC11 promoted gastric cancer cell proliferation, migration and invasion in vitro by regulating cell cycle pathway, Cell Cycle 17 (2018) 1886–1900.
[41] A. Feng, L. He, T. Chen, M. Xu, A novel cuproptosis-related lncRNA nomogram to improve the prognosis prediction of gastric cancer, Front. Oncol. 12 (2022) 957966.
[42] L. Luo, L. Li, L. Liu, et al., A necroptosis-related lncRNA-based signature to predict prognosis and probe molecular characteristics of stomach adenocarcinoma, Front. Genet. 13 (2022) 833928.
[43] J. Wang, B. Wang, B. Zhou, et al., A novel immune-related lncRNA pair signature for prognostic prediction and immune response evaluation in gastric cancer: a bioinformatics and biological validation study, Cancer Cell Int. 22 (2022) 69.
[44] Z. Wang, L. Cao, S. Zhou, et al., Construction and validation of a novel pyroptosis-related four-lncRNA prognostic signature related to gastric cancer and immune infiltration, Front. Immunol. 13 (2022) 854785.
[45] W. Wang, Q. Pei, L. Wang, et al., Construction of a prognostic signature of 10 autophagy-related lncRNAs in gastric cancer, Int. J. Gen. Med. 15 (2022) 3699–3710.
[46] J. Wei, Y. Zeng, X. Gao, T. Liu, A novel ferroptosis-related lncRNA signature for prognosis prediction in gastric cancer, BMC Cancer 21 (2021) 1221.
[47] Z. Zha, P. Zhang, D. Li, et al., Identification and construction of a long noncoding RNA prognostic risk model for stomach adenocarcinoma patients, Dis. Markers 2021 (2021) 8895723.
[48] N. Li, H. Zhang, K. Hu, J. Chu, A novel long non-coding RNA-based prognostic signature for renal cell carcinoma patients with stage IV and histological grade G4, Bioengineered 12 (2021) 6275–6285.
[49] L. Shen, N. Li, Q. Zhou, et al., Development and validation of an autophagy-related LncRNA prognostic signature in head and neck squamous cell carcinoma, Front. Oncol. 11 (2021) 743611.
[50] L. Zhang, L. Li, Y. Zhan, et al., Identification of immune-related lncRNA signature to predict prognosis and immunotherapeutic efficiency in bladder cancer, Front. Oncol. 10 (2020) 542140.
[51] K. Li, A. Zhang, X. Li, et al., Advances in clinical immunotherapy for gastric cancer, Biochim. Biophys. Acta Rev. Canc 1876 (2021) 188615.
[52] R.M. Samstein, C.H. Lee, A.N. Shoushtari, et al., Tumor mutational load predicts survival after immunotherapy across multiple cancer types, Nat. Genet. 51 (2019) 202–206.
[53] G.M. Boukhaled, S. Harding, D.G. Brooks, Opposing roles of type I interferons in cancer immunity, Annu. Rev. Pathol. 16 (2021) 167–198.
[54] M. Hagiwara, A. Fushimi, A. Bhattacharya, et al., MUC1-C integrates type II interferon and chromatin remodeling pathways in immunosuppression of prostate cancer, OncoImmunology 11 (2022) 2029298.
[55] V. Sidarala, R. Veluthakal, K. Syeda, A. Kowluru, EHT 1864, a small molecule inhibitor of Ras-related C3 botulinum toxin substrate 1 (Rac1), attenuates glucose-stimulated insulin secretion in pancreatic beta-cells, Cell. Signal. 27 (2015) 1159–1167.
[56] M. Benoist, R. Palenzuela, C. Rozas, et al., MAP1B-dependent Rac activation is required for AMPA receptor endocytosis during long-term depression, EMBO J. 32 (2013) 2287–2299.
[57] S.A. Golden, D.J. Christoffel, M. Heshmati, et al., Epigenetic regulation of RAC1 induces synaptic remodeling in stress disorders and depression, Nat. Med. 19 (2013) 337–344.
[58] Z. Zhu, Z. Yu, Z. Rong, et al., The novel GINS4 axis promotes gastric cancer growth and progression by activating Rac1 and CDC42, Theranostics 9 (2019) 8294–8311.